FULL PAPER

Molecular insights into bulk and porous κ²*P,N*-PTA metal-organic polymers by simultaneous Raman spectroscopy and inelastic neutron scattering

Franco Scalambra,[a] Svemir Rudić[b] and Antonio Romerosa[a]*

Abstract: Simultaneous Raman spectroscopy and inelastic neutron scattering have been used to obtain structural information about the isomeric metal-organic polymers *trans*-[{RuCp(PTA)$_2$-μ-CN-1κ*C*:2κ^2*N*-RuCp(PTA)$_2$}-μ-CoCl$_3$]$_n$·(DMSO)$_n$ (**2**), *cis*-{[{RuCp(PTA)$_2$-μ-CN-1κ*C*:2κ^2*N*-RuCp(PTA)$_2$}-μ-CoCl$_3$]}$_n$·{[RuCp(PTA)$_2$-μ-CN-1κ*C*:2κ^2*N*-RuCp(PTA)$_2$]Cl}$_{0.5n}$·(15H$_2$O)$_n$ (**3**) and {[{RuCp(PTA)$_2$-μ-CN-1κ*C*:2κ^2*N*-RuCp(PTA)$_2$}-μ-CoCl$_3$]}$_n$·{[RuCp(PTA)$_2$-μ-CN-1κ*C*:2κ^2*N*-RuCp(PTA)$_2$]Cl}$_{0.5n}$ (**4**) (PTA = 1,3,5-triaza-7-phosphaadamantane). Despite the complexity of the compounds, the combination of both techniques has been useful to understand the conformation-dependent fingerprint of the polymers and, at the same time, to obtain preliminary information about how the water molecules are confined in the structural channels of **3**.

Introduction

The incorporation of transition metals to polymeric moieties can give new species with mixed properties such as luminescence, flame resistance, high flexibility and redox responsivity.[1–5] Since 2005 we have presented various examples of metal-backbone polymers incorporating the ligand PTA (PTA = 1,3,5-triaza-7-phosphaadamantane) as a bidentate k^2*N,P*-linker between {RuCp}$^+$ centres.[6–9] These compounds are generally hydrophilic, form structured microparticles in water and their crystals usually amorphize under very mild conditions, so that they can be considered as a new class of materials between metal organic frameworks (MOFs) and infinite coordination polymers (ICPs).[10,11]

Recently we presented two new examples of heterometallic polymers based on the repetition unit {RuCp(PTA)$_2$-μ-CN-1κ*C*:2κ^2*N*-RuCp(PTA)$_2$}$^+$ (**1**): *trans*-[{RuCp(PTA)$_2$-μ-CN-1κ*C*:2κ^2*N*-RuCp(PTA)$_2$}-μ-CoCl$_3$]$_n$·(DMSO)$_n$ (**2**) and *cis*-{[{RuCp(PTA)$_2$-μ-CN-1κ*C*:2κ^2*N*-RuCp(PTA)$_2$}-μ-CoCl$_3$]}$_n$·{[RuCp(PTA)$_2$-μ-CN-1κ*C*:2κ^2*N*-RuCp(PTA)$_2$]Cl}$_{0.5n}$·(15H$_2$O)$_n$ (**3**). Both metal-organic polymers are constituted from dimetallic units of **1** bridged by {CoCl$_3$}$^-$ moieties via k^2*N,P* coordination of the PTA ligands. It is known that complex-cobalt units such as {CoCl$_3$}$^-$ and {Co(NCS)$_2$(H$_2$O)$_2$} can be coordinated via N atoms of the ligand PTA and its derivatives such as O=PTA.[12,13] In these complexes the coordination geometry of the cobalt is octahedral and tetrahedral but no examples of other coordination geometries have been published. In contrast, the Co coordination geometry in complexes **2** and **3** is bipyramidal-trigonal and during their synthesis and crystallization the PTA ligand does not suffer oxidation upon k*N*-coordination to the metal. This coordination can occur at opposite sides of the Ru-Ru axis of **1**, *transoid* isomer (polymer **2**), or at the same side, *cisoid* (polymer **3**) isomer (Figure 1). Crystals of **2** can be obtained from anhydrous dimethyl sulfoxide (DMSO) solutions of the polymer and are constituted from bulk, aligned chains of the polymer and monolayers of DMSO perpendicular to them. Upon addition of 10 % of water to the crystallization media, crystals of **2** undergo a significant structural modification that leads to the formation of the porous polymer **3**. Water cleaves some of the polymeric chains, leading to the isomerization of the polymer from *transoid* to *cisoid* and releasing units of the ruthenium dimer **1** which arranges perpendicular to the chains. The crystallization of PTA-metal complexes from water containing solutions used to provide crystal structures containing water molecules hosted in channels, as happens in [RuClCpPTA$_2$].[14] In this complex there is a water molecule per PTA ligand. In contrast, the crystal structure of **3** is constituted by channels containing a large amount of water molecules per PTA ligand, with cross section of approximately 14 Å x 9 Å that are filled with water molecules.[15] The study of the single crystals of **3** by X-ray diffraction evidenced that these pores contain two types of water molecules: the first are hydrogen bonded to the N$_{PTA}$ and are fixed in the outer part of the pores, while the remaining are weakly interacting with the surroundings and are found in the inner part of the pores. Under very mild conditions (23 - 80 ºC, 1 atm) all of these water molecules can be lost and the amorphous {[{RuCp(PTA)$_2$-μ-CN-1κ*C*:2κ^2*N*-RuCp(PTA)$_2$}-μ-CoCl$_3$]}$_n$·{[RuCp(PTA)$_2$-μ-CN-1κ*C*:2κ^2*N*-RuCp(PTA)$_2$]Cl}$_{0.5n}$ (**4**) is obtained.

In this work we present a study of polymers **2**, **3** and **4** by means of simultaneous Raman and inelastic neutron scattering studies (INS) performed with the TOSCA (ISIS, RAL), which is a neutron spectrometer optimized for the study of molecular vibrations in the solid state, and additionally permits recording of INS and Raman scattering simultaneously.[16] Raman

[a] F. Scalambra, A. Romerosa
Department: Áea de Química Inorgánica-CIESOL
Institution: Universidad de Almería
Address: Carretera Sacramento s/n, 04120 La Canada de San Urbano
E-mail: romerosa@ual.es
[b] S. Rudić
Department: ISIS Facility
Institution: STFC, Rutherford Appleton Laboratory
Address: Chilton, Didcot OX11 0QX, UK

Supporting information for this article is given via a link at the end of the document.

spectroscopy can give valuable information about the structure of these kind of polymers through the analysis of the vibrations of the PTA ligands, as we have recently shown for the polymer [{RuCp(PTA)$_2$-μ-CN-RuCp(PTA)$_2$}-μ-CdCl$_3$]$_n$.[9] On the other side, INS spectroscopy is very sensitive to hydrogen atoms and is not limited by selection rules, giving spectra that are dominated by all of the hydrogen related motions. In the case of polymers **2**, **3** and **4** the combination of these techniques is used herein to obtain information about the conformation of polymer **4** and to achive information on the behaviour of the water molecules nano-confined in **3**. Additionally, new procedures for synthesising the complexes are presented. In order to obtain sufficient and homogeneous amount of the polymers to perform the experiments at TOSCA, the previously published synthesis for **2** and **3**[15] has been scaled up and slightly modified. This permitted us to obtain large amount of polymers in single batches.

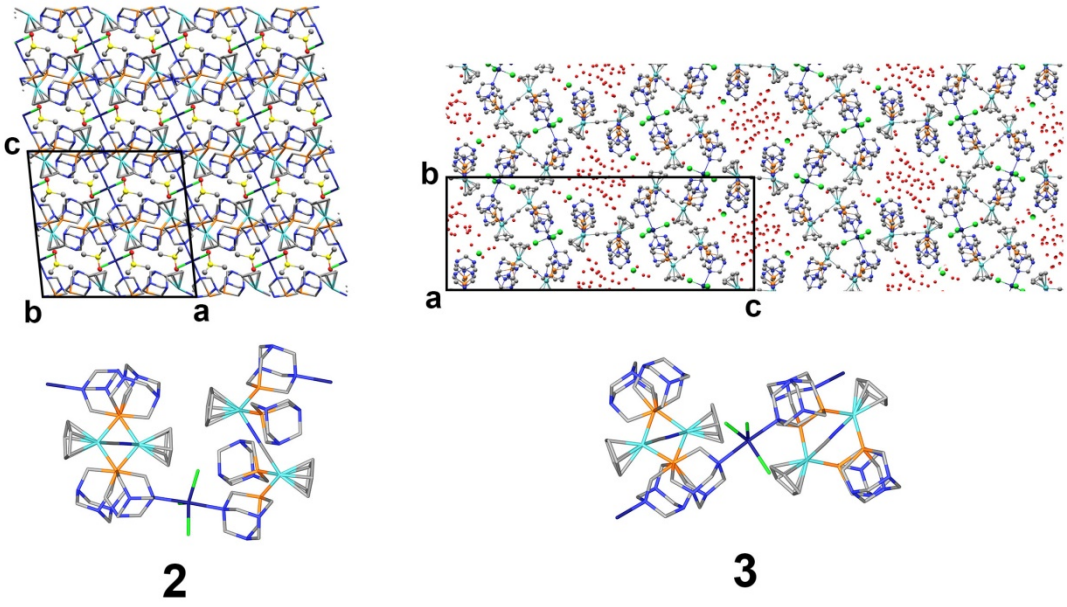

Figure 1. Conformation of adjacent monomers in the crystal structure of 2 and 3 and 2x2x2 unit cells showing their packing.

Results and Discussion

Synthesis of 2, 3 and 4.

The previously reported method to obtain **2** and **3** allows their synthesis by a procedure that was convenient to obtain these polymers in good yield in milligrams quantities. Nevertheless, such synthetic procedures are not useful to prepare grams of product, which are needed to accomplish inelastic neutron scattering studies. Thus, the published procedure for obtaining **2** and **3** needed to be scaled up to obtain ca. 2 grams of product in a single batch. The previously reported two-steps preparation for **2** has been modified to a one-step synthesis, which revealed to be faster, more robust and more efficient, providing the final product with a larger yield. Light blue crystals of **2** were obtained by reaction of anhydrous $CoCl_2$, NH_4Cl and **1** in DMSO at 100 ºC (Scheme 1). In contrast, complex **3** was synthesized by a procedure similar to that published previously but allowing for three days of reaction instead of two, which permits the complete conversion of **2** into **3** without significant increase in secondary products. Complex **4** is presented in this paper for the first time. This complex has been prepared by controlled dehydration of **3** in a solid state at 60 ºC and under reduced pressure (10^{-2} atm).

Finally, the samples were checked spectroscopically by IR spectroscopy and thermogravimetric analysis and the homogeneity of the samples was confirmed by powder X-ray diffraction.

Scheme 1. Synthesis of **2**, **3** and **4**.

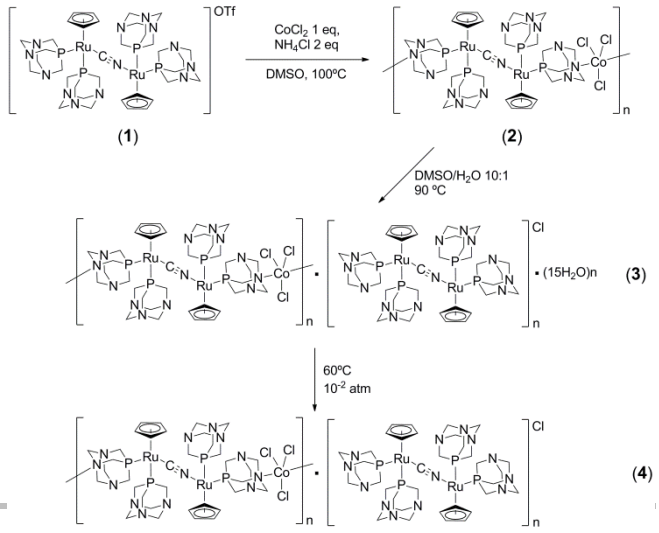

Raman Spectroscopy.

As mentioned before,[15] the crystal structures of **2** and **3** exhibit a 1D framework consisting of dimeric ruthenium units $\{(PTA)_2CpRu\text{-}\mu\text{-}CN\text{-}RuCp(PTA)_2\}^+$ linked by $\{CoCl_3\}^-$ moieties through one N atom of two different PTA ligands, resembling a *transoid* and *cisoid* conformation, respectively. The first evidence that support the polymerization of the cation **1** via N_{PTA} coordination is the shift of the C≡N stretching frequency to higher wavenumbers (**1**: 2103 cm^{-1}, **2**: 2114 cm^{-1}, **3**: 2122 cm^{-1}, **4**: 2117 cm^{-1}). Nevertheless, this information is not enough to clarify the geometry and the stoichiometry of the polymer, which can be tentatively assessed by looking at the P-C stretching, N-C stretching and breathing motions of the ligand PTA. As previously reported for the polymer $[(PTA)_2CpRu\text{-}\mu\text{-}CN\text{-}RuCp(PTA)(PTA\text{-}CdCl_3)]_n$, the bidentation of the PTA can be identified by looking at the peaks that appear in the region around 950-1150, 550-750 and 300-400 cm^{-1}. Another important feature that distinguishes the free dimeric complex **1** from its polymers is the torsional motion/frequency of the PTA ligand around 200 cm^{-1}, which arises at 194 cm^{-1} in **1** and at 205, 203 and 202 cm^{-1} in **2**, **3** and **4** respectively (Figure 2). The deconvolution of this band shows that it is composed from two components, with the higher frequency component corresponding to the bidentate PTA torsion, while the lower frequency component corresponds to the monodentate PTA torsion, as suggested by the calculated Raman spectrum of the $\{[(PTA)_2CpRu\text{-}\mu\text{-}CN\text{-}RuCp(PTA_2)]\text{-}\mu\text{-}CoCl_3\text{-}PTA\}$ fragment (Figure S22). The CH_2 rocking motions of **2** appear at ca. 340 cm^{-1}, and are overlapped with a C-S=O bending of the DMSO solvate.[17] The CH_2 rocking vibrations of **1** appear at 330 cm^{-1}, while in **3** the vibrations clearly split to give two peaks at 339 and 349 cm^{-1}. It is interesting to note that in the anhydrous polymer **4**, these vibrations join in a single broad signal centred at 339 cm^{-1} that covers the range in between 320 and 360 cm^{-1}.

The symmetric P-C stretching modes in **1** are found as a single band at 583 cm^{-1} while in **2** these modes give rise to several bands due to the PTA bis-coordination (κ^2*N,P*- PTA to Ru and Co), and are also shifted to slightly higher wavenumbers than in **1**. In **3** and **4** these motions are broader than in **2**, possibly due to the presence of intercalated **1**. The bidentation of the PTA is also evident due to the split of the N-C bending, that appears in **1** as a unique band at 656 cm^{-1}, while in **2** and **3** gives two peaks at 657, 672 cm^{-1} and 662, 676 cm^{-1}, respectively. In contrast to **2** and **3,** the same modes appear as a single broad peak in **4**, which can be due to the disordering of the polymeric chains upon dehydration. Furthermore in **2**, N-C bending region somewhat

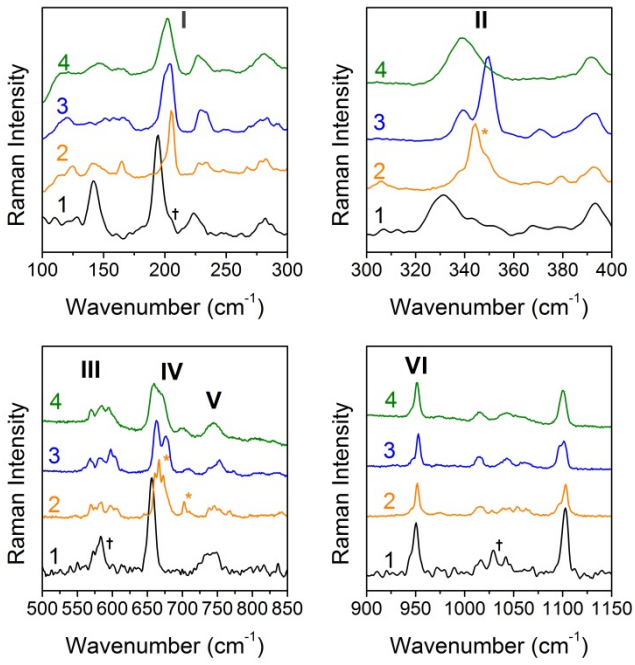

Figure 2. Selected regions of Raman spectra of **1** – **4**: Splitting of the bands relative to PTA torsion (I); CH_2 rocking motions (II); P-C stretching (III); N-C bending (IV); N-C symmetric stretching (V); N-C asymmetric stretching (V)Marked peaks correspond to DMSO (*) and $CF_3SO_3^-$ (†) vibrations.

Table 1. Significant experimental Raman vibrations of **1** – **4** and calculated vibrations of the groups in $\{[(PTA)_2CpRu\text{-}\mu\text{-}CN\text{-}RuCp(PTA_2)]\text{-}\mu\text{-}CoCl_3\text{-}PTA\}$.

	Wavenumber (cm^{-1})				
	1	**2**	**3**	**4**	Calculated (B3LYP/3-21G)[a]
τ PTA	194	205	203	202	268
ρ_r CH_2	330	338, 348	339, 349	339[b]	334
ν_s P-C	573, 578, 583	570, 575, 584, 598, 605	569, 572, 581, 598, 603	570, 584, 595	571, 579, 585, 606
δ N-C	656	657, 672	662, 676	659[b]	647, 654, 662, 676
ν_s N-C	735[b]	738, 745, 753	737, 752	744[b]	746, 756, 766
ν_{as} P-C	951	952	953	951	923
ν C≡N	2103	2114	2122	2117	2075

a) frequencies scaled by 0.965 (See SI for more information). b) broad

overlaps with the C-S antisymmetric stretching of the intercalated DMSO (667 cm^{-1}), while the C-S symmetric stretching is found at 702 cm^{-1}.[17] The N-C stretching modes appear in all of the studied compounds between 750 and 1050 cm^{-1}: symmetric stretches are centred at 745 cm^{-1}, while asymmetric stretches are centred at 952 cm^{-1}.[14]

Inelastic Neutron Scattering

Inelastic neutron scattering has been successfully used to characterize the structure and the properties of a variety of organic polymers[18–24] and metal organic frameworks.[25–28] Nevertheless, to the best of our knowledge this is the first time in which a metal-organic polymer is studied by means of this technique. The assignment of the INS peaks has been helped by comparing the experimental INS spectrum of **2** with a calculated one for a monomeric fragment (Figure 3, see also Experimental Section and Supporting Information for more details). The terahertz region of the INS spectra of **2**, **3** and **4** (see Figure 4) is composed of skeletal and lattice motions. In the range 100-350 cm^{-1} the three compounds show strong similarities, in particular the CH_2 torsions at 277 cm^{-1} do not present a significant shift or change of pattern between the three compounds. Complex **4** shows peaks at 152 and 167 cm^{-1}, which are broader than those in **2** and **3,** probably due to the disorder of the polymeric chains upon amorphization. In contrast with **3** and **4**, complex **2** also displays bands at 240 and 307 cm^{-1} that are due to the CH_3 torsions of the DMSO solvate.[29] The clearest differences among the INS spectra of the three complexes can be found between 350 and 800 cm^{-1}, where valuable information to characterize the structure of **2**, **3** and **4** can be obtained. The librations of the Cp rings appear around 350 and 390 cm^{-1} and are similar for the three compounds. In the case of the *cis* compound **3** these bands are red shifted by 2 cm^{-1} with respect to **2**. The shoulder at 404 cm^{-1} in **2** and **3** becomes a broad signal in **4**, overlapped with the peak at 392 cm^{-1} (Figure 4).

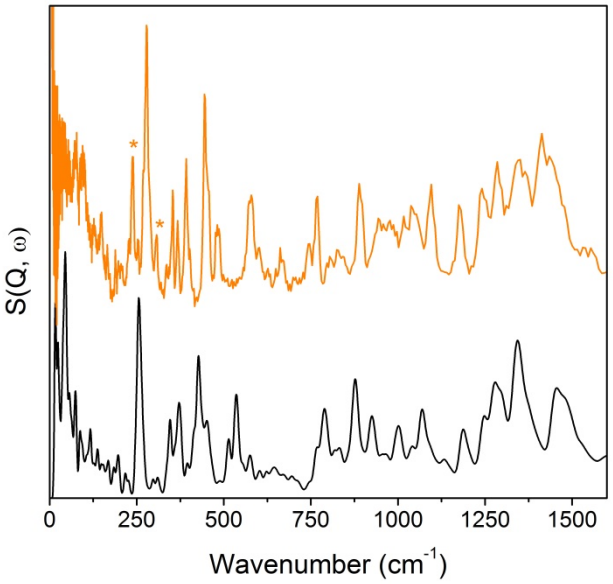

Figure 3. Experimental INS spectrum of **2** (orange trace) and calculated INS spectrum of the fragment {[$(PTA)_2$CpRu-μ-CN-RuCp(PTA_2)]-μ-$CoCl_3$-PTA} (black trace). Marked peaks correspond to DMSO (*).

The bands between 445 and 620 cm^{-1} have been assigned to CH_2-N(P)-CH_2 rocking vibrations[30,31] and they seem to be the most distinctive feature of the *trans* and *cis* isomers. Deconvolution of the peaks in this region shows that they are formed by at least three components. The pattern obtained for **2** is significantly different from that for **3**, observing respectively three components with integrals ratio of approximately 2:2:1 and 1:3:1, while for compound **4** deconvolution leads to a system

Figure 4. Region 100-800 cm^{-1} of the INS spectra of **2** (orange trace), **3** (blue trace) and **4** (green trace). torsion band of CH_2 (I); the libration of the Cp (II, III); the CH_2-N(P)-CH_2 rocking (IV, V, VI) and CH_2-N(P)-CH_2 wagging (VII). DMSO-CH_3 torsions in 2 are denoted with (*).

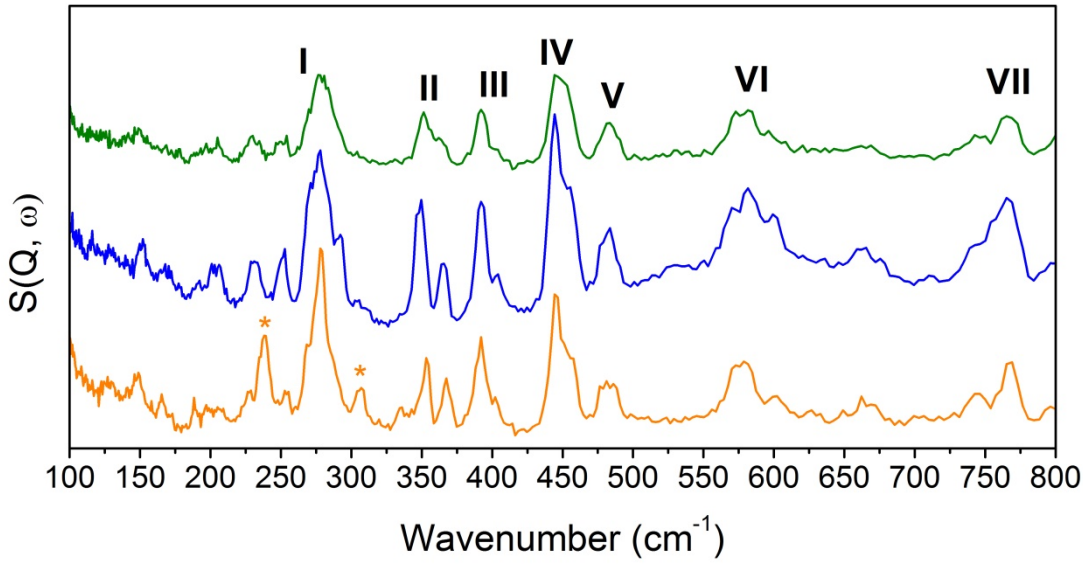

Table 2. Selected experimental INS vibrations of compounds 2-3 and calculated vibrations of the fragment {[(PTA)$_2$CpRu-μ-CN-RuCp(PTA$_2$)]-μ-CoCl$_3$-PTA}.

	Wavenumber (cm^{-1})			
	2	**3**	**4**	Calculated (B3LYP/3-21G)[a]
τ CH$_2$	278	278, 292	277	255
δ Cp	353, 367, 392, 402	350, 366, 392, 404	351, 362, 392	346, 372, 395
ρ_r CH$_2$-N(P)-CH$_2$	444, 457, 481, 573, 579, 602	444, 455, 483, 570, 582, 599	448, 483, 573, 582	415, 427, 452, 513, 536, 576
ρ_w CH$_2$-N(P)-CH$_2$	743, 769	743, 765	746, 765	766, 788

a) calculation run on fragment frequencies scaled by 0.965 (See SI for more information.

composed by four peaks with integrals ratio of 0.1:1:0.75:1 (Figure 5). The CH$_2$-N(P)-CH$_2$ wagging motions arise between 720 and 785 cm^{-1}, and their maxima are found at the same wavenumbers in all three compounds. These vibrations are related to κ*P*-PTA (745 cm^{-1}) and κ^2*N,P*-PTA (767 cm^{-1}), and have patterns that are independent from the conformation of the polymeric chains. Notably, in polymers **2** and **3**, between these peaks one can observe a shoulder at 757 cm^{-1} that in **4** is red shifted ca. 12 cm^{-1}. As mentioned in the introduction, between two chains of **2** we can find one intercalated molecule of DMSO per monomeric unit that is interacting with the N$_{PTA}$; while in **3** some of the water molecules hosted in the channels are hydrogen bonded to the N$_{PTA}$. Given that the coordination of a N$_{PTA}$ to a metal atom shifts the CH$_2$-N(P)-CH$_2$ wagging mode to higher frequencies, the N$_{PTA}$ involved in an interaction such as a hydrogen bond should also shift the band in the same direction. On this basis, the shoulder at 757 cm^{-1} found in both **2** and **3** may be tentatively assigned to the CH$_2$-N(P)-CH$_2$ wagging mode of the PTA ligands, which in **2** and **3** is interacting with the intercalated solvent (DMSO in **2**; H$_2$O in **3**).[15]

Figure 5. Enlarged view of the CH$_2$-N(P)-CH$_2$ rocking (top) and wagging (bottom) modes of **2**, **3** and **4**. The peak fitting with Gaussian curves is shown.

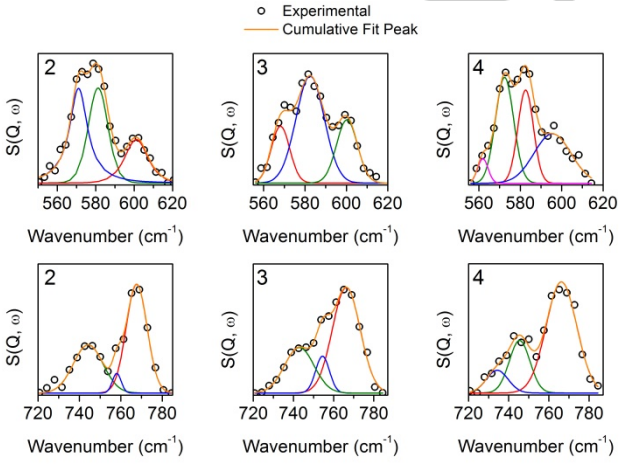

Considering that one of the aims of this study is to determine the behaviour of the intercalated water in **3**, a preliminary investigation has been done whereby the difference between INS spectra of **3** and **4** recorded at a number of temperatures (10, 50 and 100 K, see Figure 6 has been derived. The bands of the difference spectra are complicated due to the fact that in **4** the peaks are broader than in **3**, so that the subtraction does not leave a clean signal. The difference spectra can be divided into two regions: **a**) from 0 to ~300 cm^{-1}, that contains the bands of the hydrogen bonds stretching and the water translation; **b**) from ~300 cm^{-1} to ~1200 cm^{-1}, where a broad band is observed that correspond to the libration of the water molecules. The existence and position of the acoustic peak (~50 cm^{-1}) of ice I$_h$ is not so clearly visible in the 3-4 difference spectrum.

In the range **a**, the first peaks, which are observed at 79 and 124 cm^{-1} at 10 K, progressively disappear when temperature increase. The acoustic peak for ice Ih, which appears at 55 cm^{-1}, was not observed. Instead, a number of structured bands between 30 and 70 cm^{-1} (Figure 6) are observed, which can only be assigned to other polymorph of ice. Frequency range and band pattern are similar to that for ice II. Nevertheless, to confirm this hypothesis additional experiment targeted to address this specific issue are needed. The unresolved broad signal that covers the 148 – 263 cm^{-1} range presumably contains signals of the hydrogen bond stretches, that in ice I$_h$ appear at ~224 and ~296 cm^{-1}.[32] As for other systems containing nanoconfined water,[33–36] the low energy limit of the librational modes of water is found around 320 cm^{-1}. This limit is blue shifted by about 230 cm^{-1} with respect to ice I$_h$ due to the interactions of the water molecules with the host material. In the case of **3,** this fact confirms that some water molecules are H-bonded with the PTA as supported by X-ray crystallography.[15] In the range **b** of the spectrum the maximum of the librational motions at 10 K is found at ~570 cm^{-1} and does not shift upon warming to 100 K. It is known that this feature is composed by the librational modes of the water molecules around: i) the *y* axis, that corresponds to the 2_1 molecular symmetry axis and gives the component ω1; ii) the *z* axis, that is perpendicular to the molecular plane and correspond to the component ω2; iii) the *x* axis that lays in the molecular plane and corresponds to the component ω3.[32] The fact that the edge

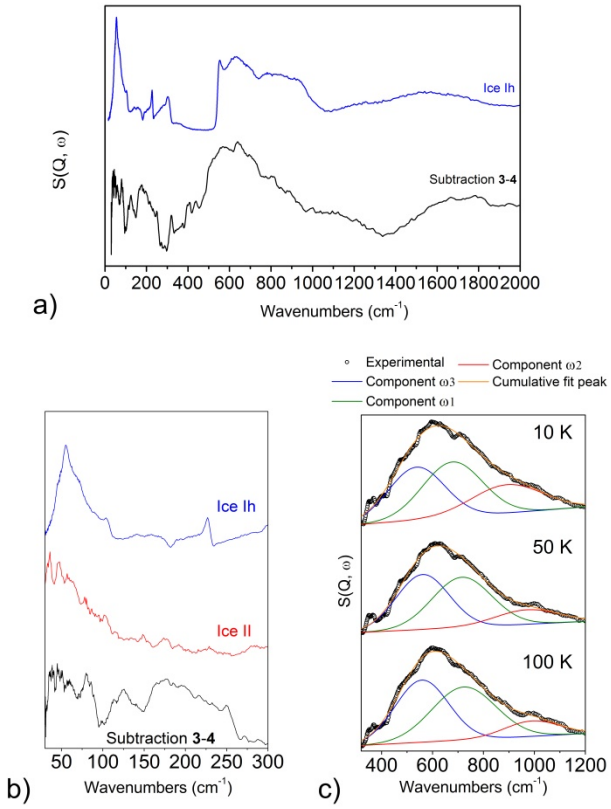

Figure 6. Left: INS difference spectrum 3-4 recorded at 10 K and INS spectrum of ice I_h. Right: expanded view of the 320-1200 cm^{-1} region of the INS difference spectra 3-4 at 10, 50 and 100 K (○) and deconvolution of the water libration bands ω1 (green trace), ω2 (red trace) and ω3 (blue trace).

of the libration bands does not shift upon warming from 10 to 100 K means that in this range of temperatures the constraint of the water molecules does not change. Furthermore, the flattening of the band ω2 upon warming from 10 to 50 K indicates that the twist motion of the water molecules becomes less hindered upon increase in temperature.

Conclusions

The metal-organic polymers **2** and **3** and the amorphized product of the latter **4** have been characterized by simultaneous Raman scattering and inelastic neutron scattering. Up to date, it is the first time that INS has been used to study such kind of molecular systems. In the Raman spectra of the studied polymers the regions of interest to recognise the κ^2*P,N*-coordination of the PTA, thus the presence of a polymeric moiety, are the ones related to: PTA torsion (ca. 200 cm^{-1}), CH_2 rocking (300-400 cm^{-1}), P-C stretching modes and N-C bending modes (550-750 cm^{-1}) and N-C stretching modes (950-1150 cm^{-1}). The information obtained from the above mentioned regions of the Raman spectra is sufficient to assess the κ^2*P,N*-coordination of the PTA, but not to clarify if the conformation of the polymer is *transoid* or *cisoid*. On the other hand, INS showed a possible key to distinguish the two isomers by looking at the CH_2-N(P)-CH_2 rocking motions of the PTA (545-620 cm^{-1}). Deconvolution and integration of the components found in this region lead to very different integral ratios in the three polymers. Additionally, INS provided a preliminary picture of the behaviour of the water nanoconfined in **3**. Subtracting the INS spectrum of **4** from the that of **3** was possible to determine the vibrations of the water molecules in **4**, which agrees well with the presence of nanoconfined water that interacts with the host porous material. The peaks found in the difference spectrum at 10 K do not shift upon rising the temperature to 100 K and the only clear difference is a flattening and broadening of the component ω2 when passing from 10 K to 50 K. This can be assigned to an augmented mobility of the water molecules around their z-axis. Additional experiments are in progress to obtain a better residual peak of the hosted water and to fully understand its behaviour in the pores of **3**.

Experimental Section

General Procedures: All chemicals were reagent grade and, unless otherwise stated, were used as received from commercial suppliers. Likewise, all reactions were carried out under pure argon by using standard Schlenk-tube techniques with freshly distilled and oxygen free solvents. Compound **4** was synthesised using the same compound **3** measured with TOSCA.

Synthesis of *trans*-[{RuCp(PTA)$_2$-μ-CN-1κ*C*:2κ^2*N*-RuCp(PTA)$_2$}-μ-CoCl$_3$]$_n$·(DMSO)$_n$ (2). Under vigorous stirring anhydrous $CoCl_2$ (571.5 mg, 4.4 mmol), NH_4Cl (471.0 mg, 8.8 mmol) and **1** (5.00 g, 4.4 mmol) were dissolved in 40 mL of DMSO at 100ºC. The solution was filtered and let to cool down to room temperature. After 24 h, the obtained light blue crystals of **2** was filtered, washed with DMSO/acetone 2:1 (3 x 30 mL), then with DMSO/acetone 1:2 (3 x 30 mL) and finally with Et_2O (3 x 30 mL). After that they have been dried in air. Yield: 3.63 g (67%).

Synthesis of *cis*-{[{RuCp(PTA)$_2$-μ-CN-1κ*C*:2κ^2*N*-RuCp(PTA)$_2$}-μ-CoCl$_3$]}$_n$·{[RuCp(PTA)$_2$-μ-CN-1κ*C*:2κ^2*N*-RuCp(PTA)$_2$]Cl}$_{0.5n}$·(15H$_2$O)$_n$ (3). Under stirring 5 g (4.1 mmol) of finely grinded crystals of **2** have been added in portions to 500 mL of a solution of DMSO/H_2O 10:1 at 90ºC. The resulting solution has been filtered while hot, and let to cool to room temperature. After 3 days, the obtained crystals of **3** have been filtered and dried on filter paper. Yield: 5.067 g (51%).

Synthesis of {[{RuCp(PTA)$_2$-μ-CN-1κ*C*:2κ^2*N*-RuCp(PTA)$_2$}-μ-CoCl$_3$]}$_n$·{[RuCp(PTA)$_2$-μ-CN-1κ*C*:2κ^2*N*-RuCp(PTA)$_2$]Cl}$_{0.5n}$ (4). After measurement on TOSCA, 2 g (0.82 mmol) of **3** have been dried under vacuum (10^{-2} atm) at 60ºC for 24 h. Yield: 1.71 g, 99 %.

Simultaneous inelastic neutron scattering (INS) and Raman measurements. Measurements were performed on the TOSCA indirect geometry time-of-flight spectrometer at the ISIS Pulsed Neutron and Muon Source (Oxfordshire, UK).[37,38] The samples were placed in a thin walled and flat aluminium cells before placement into the sample chamber which was cooled to approximately 10 K by a closed cycle refrigerator (CCR) thus reducing the impact of the Debye-Waller factor on the observed spectral intensities. INS spectra have been recorded in an energy-transfer

range of 0-8000 cm^{-1}(0-1000 meV) with a spectral resolution of $\Delta E/E$ ~1.25% i.e. 10 cm^{-1} at 800 cm^{-1}. Simultaneous Raman scattering was permitted by TOSCA probe-head design which couples the sample holder and a Raman spectrometer through an optical fibre.[16] Raman spectra have been recorder between 100-3200 cm^{-1} with a resolution between 1 and 4 cm^{-1} across the range of interest, while the laser power was 10 mW.

Computational details. DFT calculation of frequencies of a monomer have been performed at B3LYP/3-21g level of theory after geometry optimization using Gaussian 03 software package.[39,40] The conversion of the Raman vibrational modes to INS spectrum has been accomplished by a-Climax code.[41] The calculated Raman and INS spectra have been scaled by a factor of 0.965, as suggested by NIST Computational Chemistry Comparison and Benchmark Database.[42] The presented difference spectra have been smoothed by adjacent averaging to simplify the fitting of the peaks.

Acknowledgements

AR thanks “Modalidad A of Estancias de profesores e investigadores senior en centros extranjeros, incluido el Programa 'Salvador de Madariaga'," (ref: PRX16/00442; Ministerio de Educación, Cultura y Deportes) for supporting his 6-month stay at STFC Rutherford Appleton Laboratory (UK). We thank the European Commission FEDER program for co-financing the projects CTQ2015-67384-R (MINECO), the Junta de Andalucía PAI-research group FQM-317 and COST Action CM1302 (WG1, WG2). We acknowledge the beamtime awarded at the ISIS Neutron and Muon source.

Keywords: Heterometallic compounds, inelastic neutron scattering, nanoconfined water, phosphaadamantane ligands, metalorganic polymers, Ruthenium.

[1] P. Nguyen, P. Gómez-Elipe, L. Manners, *Chem. Rev.* **1999**, *99*, 1515–1548.

[2] R. P. Kingsborough, T. M. Swager, Wiley-Blackwell, **2007**, pp. 123–231.

[3] I. Manners, John Wiley & Sons., *Synthetic Metal-Containing Polymers*, Wiley-VCH, **2004**.

[4] F. S. Arimoto, A. C. Haven, *J. Am. Chem. Soc.* **1955**, *77*, 6295–6297.

[5] G. R. Whittell, M. D. Hager, U. S. Schubert, I. Manners, *Nat. Mater.* **2011**, *10*, 176–188.

[6] C. Lidrissi, A. Romerosa, M. Saoud, M. Serrano-Ruiz, L. Gonsalvi, M. Peruzzini, *Angew. Chem.* **2005**, *117*, 2624 –2628; *Angew. Chemie Int. Ed.* **2005**, *44*, 2568–2572.

[7] M. Serrano Ruiz, A. Romerosa, B. Sierra-Martin, A. Fernandez-Barbero, *Angew.Chem.* **2008**, *120*, 8793–8797; *Angew. Chemie Int. Ed.* **2008**, *47*, 8665–8669.

[8] F. Scalambra, M. Serrano-Ruiz, A. Romerosa, *Macromol. Rapid Commun.* **2015**, *36*, 689–693.

[9] F. Scalambra, M. Serrano-Ruiz, D. Gudat, A. Romerosa, *ChemistrySelect* **2016**, *1*, 901–905.

[10] A. M. Spokoyny, D. Kim, A. Sumrein, C. A. Mirkin, *Chem. Soc. Rev.* **2009**, *38*, 1218.

[11] B. Sierra-Martin, M. Serrano-Ruiz, V. García-Sakai, F. Scalambra, A. Romerosa, A. Fernandez-Barbero, *Polymers (Basel).* **2018**, *10*, 528.

[12] B. J. Frost, J. L. Harkreader, C. M. Bautista, *Inorg. Chem. Commun.* **2008**, *11*, 580–583.

[13] Ł. Jaremko, A. M. Kirillov, P. Smoleński, T. Lis, A. J. L. Pombeiro, *Inorg. Chem.* **2008**, *47*, 2922–2924.

[14] B. J. F. and, C. A. Mebi, **2004**, DOI 10.1021/OM049501+.

[15] F. Scalambra, M. Serrano-Ruiz, A. Romerosa, *Dalt. Trans.* **2018**, *47*, 3588–3595.

[16] M. A. Adams, S. F. Parker, F. Fernandez-Alonso, D. J. Cutler, C. Hodges, A. King, *Appl. Spectrosc.* **2009**, *63*, 727–732.

[17] W. N. Martens, R. L. Frost, J. Kristof, J. Theo Kloprogge, *J. Raman Spectrosc.* **2002**, *33*, 84–91.

[18] G. Goracci, A. Arbe, A. Alegría, V. García Sakai, S. Rudić, G. J. Schneider, W. Lohstroh, F. Juranyi, J. Colmenero, *Macromolecules* **2015**, *48*, 6724–6735.

[19] F. Barroso-Bujans, F. Fernandez-Alonso, S. Cerveny, S. Arrese-Igor, A. Alegría, J. Colmenero, *Macromolecules* **2012**, *45*, 3137–3144.

[20] F. Barroso-Bujans, F. Fernandez-Alonso, J. A. Pomposo, S. Cerveny, A. Alegría, J. Colmenero, *ACS Macro Lett.* **2012**, *1*, 550–554.

[21] F. Barroso-Bujans, F. Fernandez-Alonso, S. Cerveny, S. F. Parker, A. Alegría, J. Colmenero, *Soft Matter* **2011**, *7*, 7173.

[22] U. Costantino, M. Casciola, G. Pani, D. . Jones, J. Rozière, *Solid State Ionics* **1997**, *97*, 261–267.

[23] V. Crupi, A. Fontana, M. Giarola, S. Longeville, D. Majolino, G. Mariotto, A. Mele, A. Paciaroni, B. Rossi, F. Trotta, V. Venuti, *J. Phys. Chem. B* **2014**, *118*, 624–633.

[24] C. F. Araujo, M. M. Nolasco, P. J. A. Ribeiro-Claro, S. Rudić, A. J. D. Silvestre, P. D. Vaz, A. F. Sousa, *Macromolecules* **2018**, *51*, 3515–3526.

[25] Z. Lu, H. G. W. Godfrey, I. da Silva, Y. Cheng, M. Savage, P. Manuel, S. Rudić, A. J. Ramirez-Cuesta, S. Yang, M. Schröder, *Chem. Sci.* **2018**, *9*, 3401–3408.

[26] Z. Lu, H. G. W. Godfrey, I. da Silva, Y. Cheng, M. Savage, F. Tuna, E. J. L. McInnes, S. J. Teat, K. J. Gagnon, M. D. Frogley, M., Pascal, S. Rudić, A. J. Ramirez-Cuesta, T. L. Easun, S. Yang, M. Schröder, *Nat. Commun.* **2017**, *8*, 14212.

[27] M. Savage, I. da Silva, M. Johnson, J. H. Carter, R. Newby, M. Suyetin, E. Besley, P. Manuel, S. Rudić, A. N. Fitch, C. Murray, Claire, W. I. F. David, S. Yang, M. Schröder, *J. Am. Chem. Soc.* **2016**, *138*, 9119–9127.

[28] M. R. Ryder, B. Civalleri, T. D. Bennett, S. Henke, S. Rudić, G. Cinque, F. Fernandez-Alonso, J.-C. Tan, *Phys. Rev. Lett.* **2014**, *113*, 215502.

[29] L. Smrčok, D. Tunega, A. J. Ramirez-Cuesta, A. Ivanov, J. Valúchová, *Clays Clay Miner.* **2010**, *58*, 52–61.

[30] H. J. Lauter, H. Jobic, *Chem. Phys. Lett.* **1984**, *108*, 393–396.

[31] M. W. Thomas, *Chem. Phys. Lett.* **1975**, *32*, 271–273.

[32] C. Corsaro, V. Crupi, D. Majolino, S. F. Parker, V. Venuti, U. Wanderlingh, *J. Phys. Chem. A* **2006**, *110*, 1190–5.

WILEY-VCH

[33] R. T. Cygan, L. L. Daemen, A. G. Ilgen, J. L. Krumhansl, T. M. Nenoff, *J. Phys. Chem. C* **2015**, *119*, 28005–28019.

[34] N. W. Ockwig, J. A. Greathouse, J. S. Durkin, R. T. Cygan, L. L. Daemen, T. M. Nenoff, *Society* **2009**, 8155–8162.

[35] V. Crupi, D. Majolino, P. Migliardo, V. Venuti, *J. Phys. Chem. B* **2002**, *106*, 10884–10894.

[36] N. W. Ockwig, R. T. Cygan, M. A. Hartl, L. Daemen, T. M. Nenoff, *J. Chem. Phys. C* **2008**, *112*, 13629.

[37] S. F. Parker, F. Fernandez-Alonso, A. J. Ramirez-Cuesta, J. Tomkinson, S. Rudic, R. S. Pinna, G. Gorini, J. Fernández Castañon, *J. Phys. Conf. Ser.* **2014**, *554*, 012003.

[38] R. S. Pinna, S. Rudić, S. F. Parker, J. Armstrong, M. Zanetti, G. Škoro, S. P. Waller, D. Zacek, C. A. Smith, M. J. Capstick, D. J. McPhail, D. E. Pooley, G. D. Howells, G. Gorini, F. Fernandez-Alonso, *Nucl. Instruments Methods Phys. Res. Sect. A Accel. Spectrometers, Detect. Assoc. Equip.* **2018**, *896*, 68–74.

[39] A. Szabo, N. S. Ostlund, *Modern Quantum Chemistry : Introduction to Advanced Electronic Structure Theory*, Dover Publications, **1996**.

[40] A. D. Becke, *J. Chem. Phys.* **1993**, *98*, 1372–1377.

[41] A. J. Ramirez-Cuesta, *Comput. Phys. Commun.* **2004**, *157*, 226–238.

[42] "CCCBDB listing of precalculated vibrational scaling factors," can be found under https://cccbdb.nist.gov/vibscalejust.asp, **n.d.**

WILEY-VCH

FULL PAPER

A bulk and a porous metal-organic polymers based on the ruthenium dimetallic repeating unit {RuCp(PTA)$_2$-μ-CN-1κ*C*:2κ^2*N*-RuCp(PTA)$_2$}$^+$ have been characterized for the first time by Raman spectroscopy and inelastic neutron scattering, evidencing the key features of their vibrations.

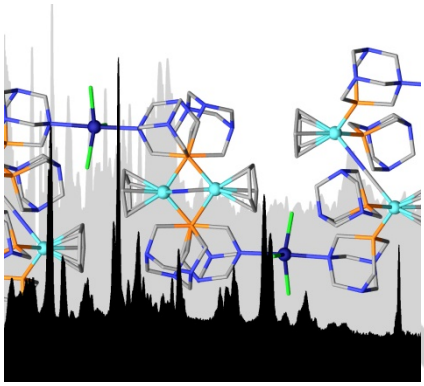

Franco Scalambra,[a] Svemir Rudić[b] and Antonio Romerosa[a]*

Page No. – Page No.

Molecular insights into bulk and porous κ^2*P,N*-PTA metal-organic polymers by simultaneous Raman spectroscopy and inelastic neutron scattering

WILEY-VCH